Catal Lett (2009) 127:406–410
DOI 10.1007/s10562-008-9710-3

Low-Temperature CO Oxidation of Gold Catalysts Loaded on Mesoporous TiO_2 Whisker Derived from Potassium Dititanate

Yinhua Zhu · Wei Li · Yaxin Zhou · Xiaohua Lu · Xin Feng · Zhuhong Yang

Received: 16 June 2008 / Accepted: 26 September 2008 / Published online: 11 November 2008

Abstract Mesoporous TiO_2 whisker was loaded with gold (denoted as Au/T(*t*), *t* represents the calcination temperature of support) by deposition-precipitation with urea (DPU) and then used in low-temperature CO oxidation. Disparate morphologies were obtained for the gold deposited on different TiO_2 whisker samples while the particle sizes were in a similar range. The better performance of Au/T(600) than Au/T(300) was attributed to the increased contacting area of gold/titania and the strong interaction between gold and well-crystallized suppot surface.

Keywords Gold · Mesoporous TiO_2 whisker · CO oxidation · Catalyst

1 Introduction

Gold catalysis has become a rapidly developing topic in chemistry these years in view of its potential applications in CO oxidation [1] and other important reactions [2–4]. Although it is generally agreed that the catalytic activity of gold catalysts depends on the particle size of deposited gold, the nature of the catalyst support has played an important role [5]. Because of high reactivity and possible strong metal support interaction (SMSI) effects [6], titania is thought to be the most prominent one among several supports and commercial titania such as P25 (Degussa AG) is mostly used as the support of Au/TiO_2 catalyst. These titania supports mainly consist of nonporous particles and own rather low surface areas, however, mesoporous titania materials which can offer large surface areas and proper nano-scale channels are very suitable to act as support of the nano-gold catalysts for its obvious quantum effect. Nevertheless, the low thermal stability, elaborate synthetic procedures and more importantly the low crystallinity together result in unstable catalytic performances which prevent the mesoporous titania from being a qualified gold catalyst support. In our earlier work, a mesoporous titania was synthesized using a novel template-free method [7]. The mesoporous titania owned not only a high thermal stability [7] (a high specific surface area of 139 m^2/g was maintained after calcination at 500 °C for 2 h) but also a same crystallographic orientation for all composed titania nanoparticles [7]. Besides, the mesoporous titania support has a special whisker morphology, which was thought to come out widely different catalytic performances [8–11]. For example, disparate catalytic activities were obtained for CeO_2 nanorods and nanoparticles [8, 9], TiO_2 nanofibers [10] and porous α-Fe_2O_3 nanorods [11] when used as the support of gold catalyst. Our recent study also showed that the Pt-doped TiO_2 whisker catalyst had a high activity in photocatalytic degradation of organics [12–15] which directly indicates the application potential of TiO_2 whisker as an excellent catalyst support of noble metals. In the present paper, the TiO_2 whisker is firstly loaded with gold by homogeneous deposition-precipitation method and tested in the low-temperature CO oxidation reaction to investigate its suitability of acting as gold catalyst support.

2 Experimental

2.1 Preparation of TiO_2 Whisker Support and Catalysts

TiO_2 whisker was prepared following the procedure: Potassium dititanate whisker ($K_2Ti_2O_5$) was synthesized

Y. Zhu · W. Li · Y. Zhou · X. Lu (✉) · X. Feng · Z. Yang
State Key Laboratory of Materials-oriented Chemical Engineering, Nanjing Uinversity of Technology, Nanjing 210009, People's Republic of China
e-mail: xhlu@njut.edu.cn

first as our previous works [16]. The dried acid-washed protonic titanate was obtained [7] and then calcined at 300 and 600 °C, respectively, for 2 h to get two TiO_2 whisker samples. Gold (1.0 wt%) was deposited on as-synthesized TiO_2 whisker samples by DPU method. In a typical procedure, excess urea (3.78 g) was dissolved in 150 mL of 0.52 mmol/L $HAuCl_4$ solution at room temperature. About 1.5 g titania support was then added into the yellow solution, the resulting mixture was heated at 80 °C for 2 h under vigorous stirring. The suspension was then cooled down and filtered, followed by washing several times with distilled water. The solid product was oven-dried at 60 °C for 12 h and calcined at 300 °C for 2 h in static air before activity evaluation. For comparison, commercial titania (P25, Degussa Co.) was loaded with gold following the same procedure. ICP-AES results showed that the gold loadings were 1 wt% for all the prepared catalysts.

2.2 Catalyst Characterization

TiO_2 whisker support together with the precursor potassium dititanate whisker and intermediate ion-exchange product were all characterized by X-ray diffraction (Bruker D8), CuKα radiation with a nickel filter was used, operating at 40 kV and 30 mA. The morphology and structure of the samples were investigated using scanning electron microscope (SEM, FEIQUANTA-200) and transmission electron microscope (TEM, JECS-2100). The textural properties were studied by N_2 adsorption–desorption measurements at liquid nitrogen temperature (BELSORP II-mini). Before analysis, the samples were degassed for 2 h at 150 °C in vacuum.

2.3 Catalytic Activity Tests

The reactions were carried out in a fixed-bed reactor using 50 mg gold catalyst for each sample. The reactant gas (1 vol.% CO and 1.98 vol.% O_2 balanced with helium) was admitted at a flow rate of 20 mL/min, corresponding to a space velocity of 24 $Lh^{-1}g_{cat}{}^{-1}$. The flow rate of reactant gas was monitored by mass flow controllers. The temperature was controlled by a thermocouple placed inside the catalyst bed. The effluent gas was analyzed with an HP-6890 gas chromatograph equipped with a thermal conductivity detector (TCD) and a molecular 13× column using helium as the carrier gas.

3 Results and Discussion

3.1 Structural Properties of the Catalysts

The phase constitutions of TiO_2 whisker and its precursors were shown in Fig. 1. The (001) peak was the strongest

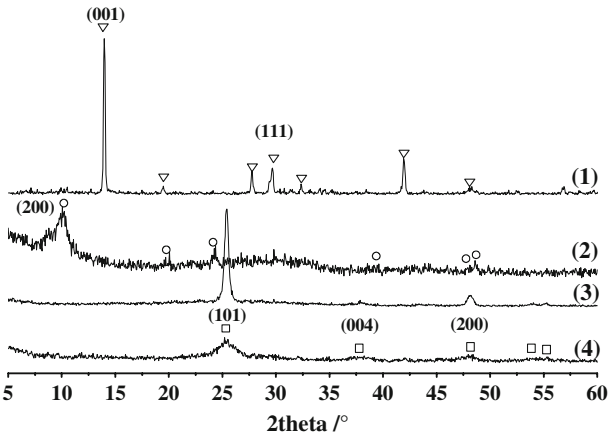

Fig. 1 XRD patterns of (1) potassium titanate precursor, (2) ion-exchanged product, (3) Au/T(600), (4) Au/T(300). (▽) $K_2Ti_2O_5$, (○) $H_2Ti_2O_5{\cdot}H_2O$, (□) anatase

peak in the XRD pattern of potassium titanate precursor and the intensity of the (111) peak was only about one-fifth that of the (001) peak, which corresponded with the oriented growth of $K_2Ti_2O_5$ [17]. After K^+ was totally removed by acid washing, the product was composed of titanate $H_2Ti_2O_5 \cdot H_2O$ (JCPDS 47-0124) which was confirmed by the peaks at $2\theta = 9.7°$ and 24.1°. Further investigation showed that all the diffraction peaks for the Au/T(t) samples can be indexed to (101), (004), (200), (105) and (211) peaks, corresponding to anatase type TiO_2 (JCPDS 21-1272). No rutile type TiO_2 were detected for Au/T(600), indicating an high phase stability of the anatase type titania support. The XRD patterns also displayed no gold peaks which might be attributed to the high dispersion of gold and/or the very low gold loading. Moreover, the relative intensity of the (101) plane for TiO_2 whisker was much higher compared with that for commercial titania P25. According to the literature [18], the preferential exposed plane determined by the shape of the particles should be the reason.

N_2 adsorption–desorption isotherms of the mesoporous titania whisker samples were shown in Fig. 2a. The ion-exchanged protonic titanate had a lower N_2 adsorption amount than its two calcined products and its isotherm was typical of type I, indicating the protonic titanate being a microporous material. The calcination temperature considerably influenced the isotherms. The isotherm of T(300) was a combination of type I and IV with two distinct regions: at low relative pressures, the isotherm exhibited high adsorption, indicating that T(300) contained micropores, at high relative pressures from 0.45 to 0.95, the isotherm had hysteresis loop of type H4, indicating the presence of mesopores in T(300). Therefore, T(300) sample was a micro-mesoporous material. However, after calcined at 600 °C, the isotherm shape was converted to

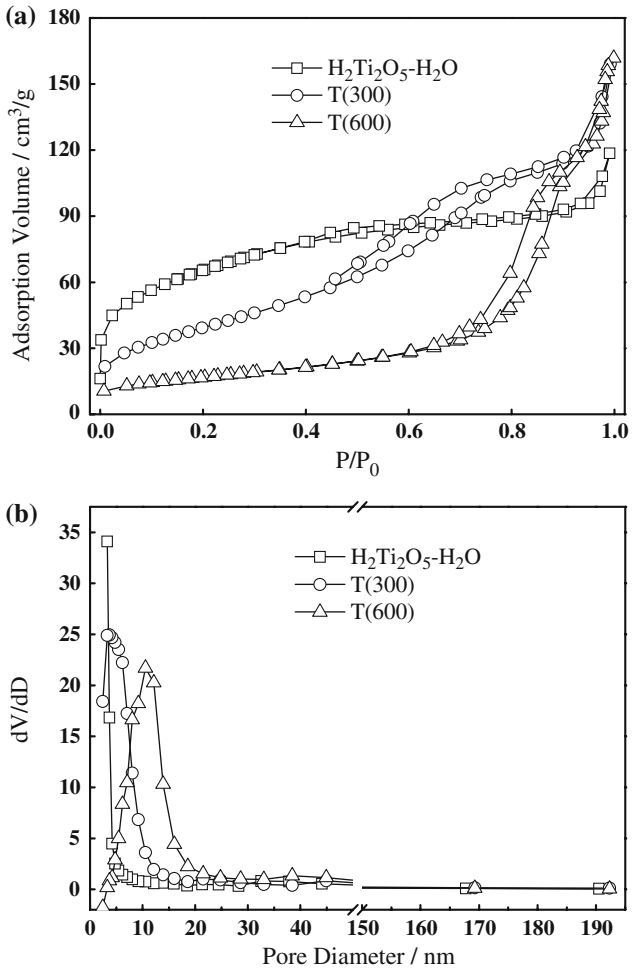

Fig. 2 N_2 adsorption–desorption isotherms **a** and pore size distributions **b** of $H_2Ti_2O_5 \cdot H_2O$ and T(*t*) samples

the one of type IV, indicating the disappearance of micropores and the formation of pure meso-structure during the calcination. These results were also proved by the pore size distributions of these samples calculated by applying the BJH approach to the desorption branches of the corresponding isotherms, as shown in Fig. 2b.

Although the pore size distributions of all the samples were relatively narrow, they were widely different from each other. Table 1 summarized the physical properties of the samples. Higher calcination temperatures resulted in both lower BET areas and larger BJH pore diameters. Specifically, the BET area of the T(600) sample was 59 m^2/g, slightly higher than commercial P25 (50 m^2/g), indicating a high thermal stability. And no evident difference was observed after loading gold for the structural properties of both Au/T(*t*) samples which meant that the micro or meso-scale structures of the samples were all well preserved.

Scanning electron microscopy (SEM) images of Au/T(*t*) samples were shown in Fig. 3a, b. The morphologies in the

Table 1 Chemical component and physical properties of the samples

Sample	Crystal phase	BET surface area/m^2/g	BJH pore diameter/nm	Pore volume/cm^3/g
P25	Anatase + Rutile	50	–	–
$H_2Ti_2O_5 \cdot H_2O$	–	237	3.3	0.08
T(300)	Anatase	143	3.7	0.24
Au/T(300)	Anatase	141	3.9	0.24
T(600)	Anatase	59	11.0	0.23
Au/T(600)	Anatase	55	11.0	0.24

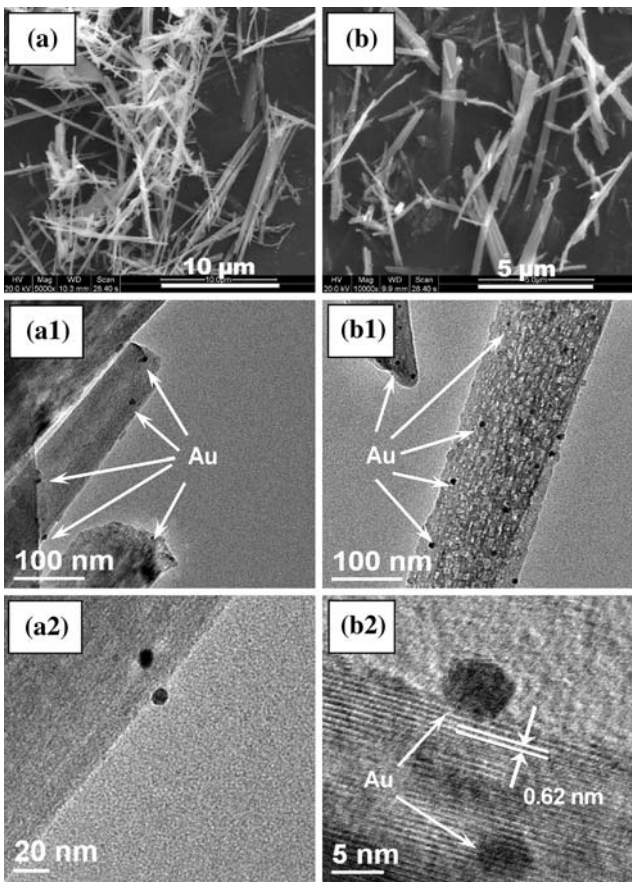

Fig. 3 SEM **a**, **b** and TEM images (**a**1, **a**2, **b**1, **b**2) of Au/T(300) (**a**, **a**1, **a**2) and Au/T(600) (**b**, **b**1, **b**2) after calcination at 300 °C (2 h, Static Air)

micrometer scale of TiO_2 whisker were well preserved after loading gold. Most of the products in "a" and "b" were whiskers with uniform size and good whisker morphology, their average diameters were 0.3, 0.6 μm respectively and their average lengths were all >5 μm. A deep insight into the fine structure of Au/T(*t*) samples can be obtained by TEM observations. Figure 3 (a1, b1) showed the larger scale TEM images which revealed that the nanoparticles were undoubtedly deposited on the

supports. Another obvious phenomenon was that the supports owned two widely different surface morphologies. Specifically, the surface of Au/T(600) was much rougher than that of Au/T(300), and it was also revealed that the support material of Au/T(600) was composed of close-packed bright spots of 5–15 nm in diameter which could be corresponded to the mesopores of the titania support regarding its pore size data listed in Fig. 2 and Table 1. Similar to Au/T(600), a few less brighter spots also existed on the surface of T(300) which was consistent with the microstructural transformation in the dehydration process of the protonic titanate. Noting that the protonic titanate ($H_2Ti_2O_5 \cdot H_2O$) was composed of massive micropores and owned a high surface area, the growth of TiO_2 crystallites was accompanied with the collapse of the micropores which resulted in the increase of pore diameter and the decrease of specific surface area.

Although the specific surface area of T(300) was much higher than that of T(600) as mentioned above, the gold nanoparticles were not as well-dispersed as expected on T(300). Remarkably, similar gold particle size distributions of Au/T(*t*) samples were observed with a gold particle size of 8.5–13.5 and 6.5–11.5 nm for Au/T(300) and Au/T(600) respectively, which was much larger than those obtained in the literatures [19, 20]. That must be attributed to the different preparation conditions. And it was difficult to find a large number of gold particles due to the low gold loading or more probably the poor gold dispersions. Interestingly, these two gold particle sizes were very similar to the BJH pore diameter of T(600) and distinctly larger than that of T(300) (shown in Table 1). Moreover, it was found that each gold nanoparticle was embedded in one mesopore (bright spots in Fig. 3b1) of the T(600) support. This special way of combination must increase the contacting area between gold nanoparticles and the T(600) support, which was usually thought to be crucial to the catalytic activity. Claus and coworkers found that the support influences the morphology of the gold nanoparticle: more-rounded gold particles were present on TiO_2, while highly faceted particles were present on ZrO_2 [21]. In this work, HRTEM images (Fig. 3a2, b2) furthermore revealed different gold particle morphologies on the two supports. For gold particles on T(300), a rather rounded morphology was observed while the particles presented a highly faceted hexagonal shape on T(600). This might be attributed to the stronger interaction between gold nanoparticles and T(600) support than that on T(300). Though the periphery of the particle bounded on the support was not clearly visible in Fig. 3b2, it was these peripheral atoms that were responsible for the activation of dioxygen in the catalytic process. In addition, the titania whisker support owned a well crystallized structure with the lattice fringe corresponding to a *d* spacing of 0.62 nm (Fig. 3b2), which might be beneficial to its catalytic performance.

3.2 Catalytic Activity of the Prepared Catalysts

The catalytic activity of the Au/T(*t*) catalysts in low temperature CO oxidation reaction, measured in the temperature range of 20–160 °C, was presented in Fig. 4. Au/T(600) owned the best catalytic activity among all the prepared gold catalysts including Au/P25. Specifically, the 100% CO conversion for Au/T(600) was reached at 80 °C while 120 °C was needed for Au/T(300). Additionally, it could be found that $T_{50\%}$ (temperature for 50% conversion) for Au/T(300), Au/T(600) and Au/P25 catalysts were about 50, 30 and 40 °C respectively, indicating a same activity order. There is no doubt that a high surface area will be beneficial to the dispersion of gold particles, but the highest activities were often obtained with supports having moderate surface areas [22]. In our experiments, TiO_2 whisker with a higher surface area did not come out a better performance, which had no conflict with literature's result [22]. To find out the reason of this phenomenon, other factors related to the nature of support such as surface roughness, degree of crystallinity and pore size distribution were took into consideration. All of these factors affect the size and shape, the electronic states of deposited gold particles, which further influence the catalytic performance. For example, Wang et al. [23] ascribed the enhanced catalytic activity of the Au/MnO_2 catalyst to the surface oxygen vacancies resulting from the strong interaction between Au and the MnO_2 support. Yan et al. [24] found that brookite supported gold catalyst showed a higher stability against sintering compared with anatase, which resulted from the unique surface properties of brookite. In the present work, the mesopores of T(600) provided plenty of anchoring sites for gold nanoparticles which were different from the situation of T(300),

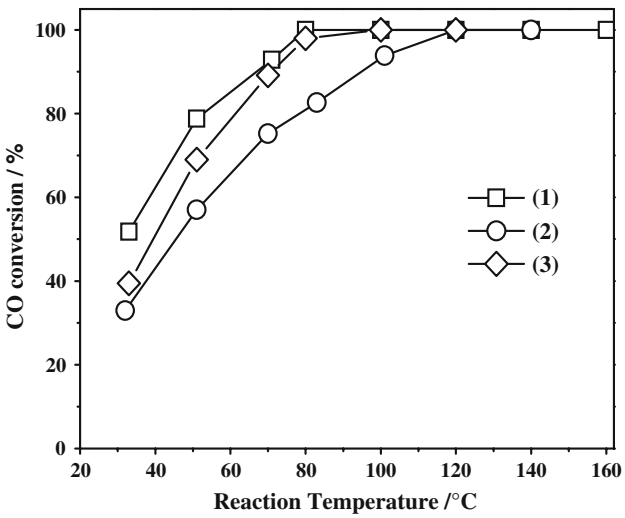

Fig. 4 Effect of different titania support on the CO conversion. (1) Au/T(600); (2) Au/T(300); (3) Au/P25

considering the gold particle size and the pore diameter of support. Noting that the TiO_2 whisker can maintain its anatase polymorph after calcination at 600 °C, a high crystallinity titania surface was obtained in the meantime, which could be confirmed by the HRTEM image (Fig. 3b2). To the best of our knowledge, the synthesis of stable titania with high crystallinity and large surface area is still a challenge, the mesoporous titania whisker might be a good support for noble metals. Our result also showed that strong interactions might exist between gold nanoparticles and the well-crystallized support surface of Au/T(600), which resulted in a higher faceted gold morphology compared with Au/T(300). Moreover, we can also imagine that the mesopores of T(600) were crucial to stabilize the nanoparticles and also to enlarge accessible interface area for the similar pore size with the deposited gold particles. This hypothesis could be easily confirmed by introducing an accepted fact: The higher activity observed with the Au/TiO_2 catalysts was associated with the more-rounded morphology of the particles accompanied by a higher relative amount of low-coordinate surface sites [25]. Catalyst with more-rounded gold nanoparticles was less active than that with faceted gold particles in this work. Considering the very similar gold particle sizes, the most reasonable explanation of the catalytic performances was that the available interface area of Au/T(300) was distinctly smaller than that of Au/T(600) due to the improper pore size. Besides activity, the thermal stability should be another important factor for application. The high anatase stability of TiO_2 whisker might enhance the durability of the catalyst. Moreover, the titania support with the special whisker morphology studied in this work might exhibit some good properties in other fields, which is still under investigation.

In summary, we have successfully prepared Au/T(t) catalysts by DPU method using mesoporous TiO_2 whisker calcined at different temperatures as supports. The structural properties of the mesoporous TiO_2 whisker changed obviously with the calcination temperature. Totally different gold particle morphologies were obtained on the two different TiO_2 whisker supports while the gold particle sizes were similar. The catalytic tests show that the gold supported on T(600) is much more active than that on T(300), which is attributed to the increased contacting area of gold/titania and the collaborative effects resulting from the strong interaction between gold nanoparticles and the well crystallized support surface.

Acknowledgments This work is supported by the NSFC (20676062, 20736002, 20706029 and 20706028), 863 project (2006AA03Z455), the KSF of Jiangsu Province (BK 2007051). The authors also thank Professor Liu Xiaoheng (Nanjing University of Science and Technology) for providing the TEM measurements.

References

1. Haruta M, Yamada N, Kobayashi T, Iijima S (1989) J Catal 115:301
2. Kung HH, Kung MC, Costello CK (2003) J Catal 216:425
3. Corma A, Serna P (2006) Science 313:332
4. Yamada M, Kawana M, Miyake M (2006) Appl Catal A 302:201
5. Comotti M, Li WC, Spliethoff B, Schuth F (2006) J Am Chem Soc 128:917
6. Tauster SJ, Fung SC, Garten RL (1978) J Am Chem Soc 100:170
7. M He, XH Lu, X Feng, L Yu and ZH Yang (2004) Chem Commun 2202
8. Yuan ZY, Idakiev V, Vantomme A, Tabakova T, Ren TZ, Su BL (2008) Catal Today 131:203
9. Huang PX, Wu F, Zhu BL, Gao XP, Zhu HY, Yan TY, Huang WP, Wu SH, Song DY (2005) J Phys Chem B 109:19169
10. Zhu BL, Li KR, Feng YF, Zhang SM, Wu SH, Huang WP (2007) Catal Lett 118:55
11. Zhong Z, Ho J, Teo J, Shen S, Gedanken A (2007) Chem Mat 19:4776
12. Yang ZH, Bao NZ, Zheng Z, Liu C, He M, Feng X, Lu XH (2002) Chin J Catal 23:539
13. Yang ZH, Bao NZ, Liu C, Feng X, Xie JW, Ji XY, Lu XH (2002) Chem J Chinese U 23:1371
14. Shi YP, Yang ZH, Feng X, Zheng Z, Lu XH (2003) Chin J Catal 24:663
15. Zhou XF, Li W, Zheng Z, He M, Yang ZH, Feng X, Lu XH (2007) Chin J Catal 28:327
16. Bao NZ, Feng X, Lu XH, Shen LM, Yanagisawa K (2004) AIChE J 50:1568
17. Liu C, He M, Lu XH, Zhang QT, Xu ZZ (2005) Cryst Growth Des 5:1399
18. Xu R, Wang X, Wang DS, Zhou KB, Li YD (2006) J Catal 237:426
19. Zanella R, Giorgio S, Henry CR, Louis C (2002) J Phys Chem B 106:7634
20. Zanella R, Giorgio S, Shin CH, Henry CR, Louis C (2004) J Catal 222:357
21. Hashmi ASK, Hutchings GJ (2006) Angew Chem Int Edit 45:7896
22. Moreau F, Bond GC (2007) Catal Today 122:215
23. Wang LC, Liu YM, Chen M, Cao Y, He HY, Fan KN (2008) J Phys Chem C 112:6981
24. WF Yan, B Chen, SM Mahurin, S Dai and SH Overbury (2004) Chem Commun 1918
25. Mohr C, Hofmeister H, Claus P (2003) J Catal 213:86